We are IntechOpen, the world's leading publisher of Open Access books
Built by scientists, for scientists

6,900
Open access books available

185,000
International authors and editors

200M
Downloads

154
Countries delivered to

Our authors are among the

TOP 1%
most cited scientists

12.2%
Contributors from top 500 universities

BOOK CITATION INDEX
CLARIVATE ANALYTICS
INDEXED

WEB OF SCIENCE™

Selection of our books indexed in the Book Citation Index
in Web of Science™ Core Collection (BKCI)

Interested in publishing with us?
Contact book.department@intechopen.com

Numbers displayed above are based on latest data collected.
For more information visit www.intechopen.com

PEM-Less Microbial Fuel Cells

Reuben Y. Tamakloe

Additional information is available at the end of the chapter

Abstract

Microbial fuel cells (MFCs) are comparatively new technique of simultaneously generating electricity from bio-waste while degrading the organic waste. The use of microbes to generate electricity is an uninterrupted process in MFCs since the bacteria replicate and continue to produce power indefinitely as long as there is enough food source to nurture the bacteria. Besides, MFCs have the potential to produce hydrogen for fuel cells, desalinate sea water, and provide sustainable energy sources for remote areas. Factors like type of electrodes used in the cells, partitioning of cells, oxygen complement and configurations are important factors that affect the performance of MFCs. The fabrication of microbial fuel cells of different configurations and the relationship between the factors affecting the efficiency of single chambered (SC-MFCs) and double chambered (DC-MFCs) will be presented. The experimental data on observations made on the effects of these materials on the MFCs characteristics, electricity generation and wastewater treatment have also been included. The main aim of this study is to find out whether a nonconventional inexpensive clay could be used as an ion-exchange medium alternative to the conventional expensive PEM in the fabrication of MFCs. The results obtained on power generation, current density, open circuit voltage, etc., clearly show that PEM-less MFCs can be used as practical devices for sustainable energy generation.
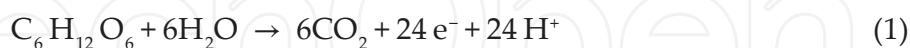
Keywords: MFC (microbial fuel cell), current density, power density, SC-MFC (single chambered MFC), DC-MFC (double chambered MFC), OCV (open circuit voltage), COD (chemical oxygen demand)

1. Introduction

The production of electricity from waste and renewable biomass using microbes has gained much attention in the recent past [1]. There are three main parts in MFCs [1, 2]. (1) An anode chamber where fuel is oxidized by microorganisms and electron as well as protons are generated. (2) A cathode chamber where electrons and protons are consumed, producing water

by combining with oxygen. (3) A cation exchange membrane (CEM) which transfers protons from anode chamber to meet with the electrons transferred through external electric circuit from anode chamber to cathode chamber [3–6]. The fuel for the cell is usually domestic or industrial wastewater which contains microorganisms and organic compounds. The reaction for the catabolic activity of the microbes may be summarized as follows:

Microbes

$$C_6H_{12}O_6 + 6H_2O \rightarrow 6CO_2 + 24\,e^- + 24\,H^+ \tag{1}$$

Reduction half reaction:

$$24\,H^+ + 24\,e^- + 6O_2 \rightarrow 12\,H_2O \tag{2}$$

Overall oxidation/reduction reaction:

$$C_6H_{12}O_6 + 6O_2 \rightarrow 6CO_2 + 6H_2O \tag{3}$$

Thus there are two halves of the microbial fuel cell: the aerobic chamber having positively charged electrode with oxygen in abundant, and the anaerobic chamber having negatively charged electrodes. The semi-permeable membrane separate the two chambers allows only hydrogen ions (H^+) and keeps oxygen out of the anaerobic chamber [7].

The main challenges in constructing microbial fuel cells (MFCs) are the identification of materials and architectures that maximize power generation and efficiency, also minimizing the cost of fabrication. Various researchers have tried to use different materials and various architectures for the electrode and membranes. In order to get better performance, a broad range of techniques have also been used [8]; which include "doping" of the anode, varying the electrodes and the use of various types of cathode substrate.

2. Advantages of PEM-less microbial fuel cells over PEM architecture

As we know, the PEM key function is to keep the liquid contents of each chamber separate while still allowing protons to pass between chambers to be utilized in the cathode with the produced electrons. Although proton exchange membranes are often used, Logan [10] has reported that Cation exchange membranes (CEM) work in a similar way but more cost effective than PEM, and sometimes structurally stronger. Both PEM and CEM support in reducing oxygen diffusion in the anode chamber of the cell. However, after using PEM for some of MFCs we have realized that PEM is quite expensive and very delicate to work with. It cannot be reused and also difficult to adapt to desired shapes.

We therefore started searching for other alternatives to replace the most costly and delicate PEM. In the process of this search we came across a local clay mixed with kaolin and bentonite and subsequently fired appropriately achieved the desired results of producing open circuit voltage (OCV) of up to 1.5 volts. This clay system is quite unique, robust, potable, cheap, easy

to acquire locally and can be shaped as desired. It can also be molded to large cells. Even though some cheaper alternatives have been used by many researchers, the use of rigid cation exchange materials such as the clay used in the fabrication of some of MFCs in this research have not been given much attention that is most cost effective and easy to give any desired shape.

3. Section A

This section includes the fabrication, operation and results of three different types of Microbial Fuel Cells (MFCs).

3.1. Single-chambered (SC-MFC) PEM microbial fuel cell

In order to find the effect of chemical oxygen demand (COD) on the open circuit voltage (OCV), Power production and coulombic efficiency single–chambered Microbial Fuel Cells (MFCs) have been fabricated. Three different MFCs of similar design have been fabricated using carbon paper doped with platinum as cathode and graphite as anode separated by Proton Exchange Membrane (PEM) and the effect of COD level on Open Circuit Voltage (OCV), power production and Coulombic efficiency have been studied.

3.2. Double-chambered (DC-MFC) PEM microbial fuel cell

A variety of substrates have been explored relative to the anode substrate which takes the form of any wastewater with some amount of COD. Several modification methods have been developed to improve power generation at the anode level, but the cathode system and configuration have also been a challenge in most researches. The choice of cathode substrate is one of the greatest challenges in fabricating MFCs. A DC-MFC with H_2O_2 cathode has been fabricated and compared with SC-MFC.

3.3. Membrane less microbial fuel cell

In this case, a number of clay mixtures have been used as ion-exchange partition replacing Proton Exchange Membrane (PEM) in designing the MFC and observations have been made on the effects of these materials on the MFCs characteristics; electricity generation and wastewater treatment. The performances of the cells have been then compared in terms of wastewater treatment, power generation and coulombic efficiency.

3.4. Methodology

3.4.1. Single-chambered (SC-MFC) PEM microbial fuel cell

3.4.1.1. Preparation of PEM

Nafion 117 of area 12.6 cm^2 was taken through the normal cleaning process [distilled water → 3% hydrogen peroxide → dilute sulfuric acid → distilled water].

3.4.1.2. Fabrication of MFCs

Necessary steps for the fabrication of MFCs:

- 2 Perspex slabs were cut, shaped and dilled for each cell.

- Carbon paper doped with platinum was cut and shaped.

- Copper conductor was cut and shaped.

- Preparation of Graphite electrode.

- A plastic container of 2 liters capacity served as the anodic chamber. The anode chamber contains the wastewater and the graphite electrode. The carbon paper tightens onto the PEM served as the cathode.

3.4.1.3. Types of wastewater for MFCs

Following three types of wastewater of different COD and pH from GGBL (Kumasi, Ghana) were used as Fuel for these cells. The characteristics of the wastewater are listed in **Table 1**:

Wastewater	COD(mg/L)	pH
Influent	3790.0	11.18
Anaerobic	748.0	6.80
Balance	4330.0	6.01

Table 1. Type of wastewater used.

3.4.1.4. Operation

The cells were kept at 25°C (±0.5°C). The anode was immersed in the wastewater such that the copper conductor did not touch the water in order to avoid corrosion. The anode chamber was sealed to maintain anaerobic system throughout the experiment. OCV readings were taken for 35 days with the CR10X datalogger which stores the differential voltage every 1 min. A multimeter (Peak Tech 2010DMM) was used in the reading of the load voltage and the current through a resistance box ranging from 0 to 10,000 Ω.

3.4.1.5. Results

The experiment was operational for 35 days. A constant increment of OCV was observed from day one of the operation of MFCs until it got to their peak values of OCV. These values were maintained for about 10 days. Also their pH and COD values at the end experiment are given in **Tables 2** and **3**. The experiments were performed with the wastewater as collected in order to check the viability of the cells without adding inoculants and other chemicals (**Figure 1**).

Wastewater	Starting COD	Ending COD	Starting pH	Ending pH
Influent	3790.0	133	11.18	8.3
Anaerobic	748.0	59	6.8	8.9
Balance	4330.0	267	6.01	8.6

Table 2. pH values obtained.

	Day 1	Day 2	Day 3	Day 4	Day 5	Day 6	Day 7	Day 8	ΔCOD	
pH	5.9	6.1	6.1	6.2	6.4	6.6	6.7	6.9		
Temp. °C	26	28	26	27	27	28	28	27		
COD (mg/L)	7700	—	—	—	—	—	—	1650	6050	78.6%

Table 3. Change in pH of the wastewater with activities of microbes through the days.

3.4.2. Double-chambered (DC-MFC) PEM microbial fuel cell

3.4.2.1. Architecture

We fabricated the DC-MFC with the porous pot (5 mm thick) containing the anodic substrate immersed into the copper can containing the H_2O_2 catholyte substrate (**Figure 2**), both having working volume of 300 mL in each compartment. The anode electrode is a zinc rod having an outer diameter of 1.2 cm and a geometric surface area of 38.8 cm^2 and the cathode is the copper can housing the porous pot (this is similar to a Daniel cell). The pot acts as an ion exchange partition. We connected the anode or the zinc rod to the cathode compartment through a copper wire and external resistor of 1000 Ω. The assumption is that the porous pot separation permit only cation transport to the oxidation substrate, as done earlier [9]. The initial pHs in
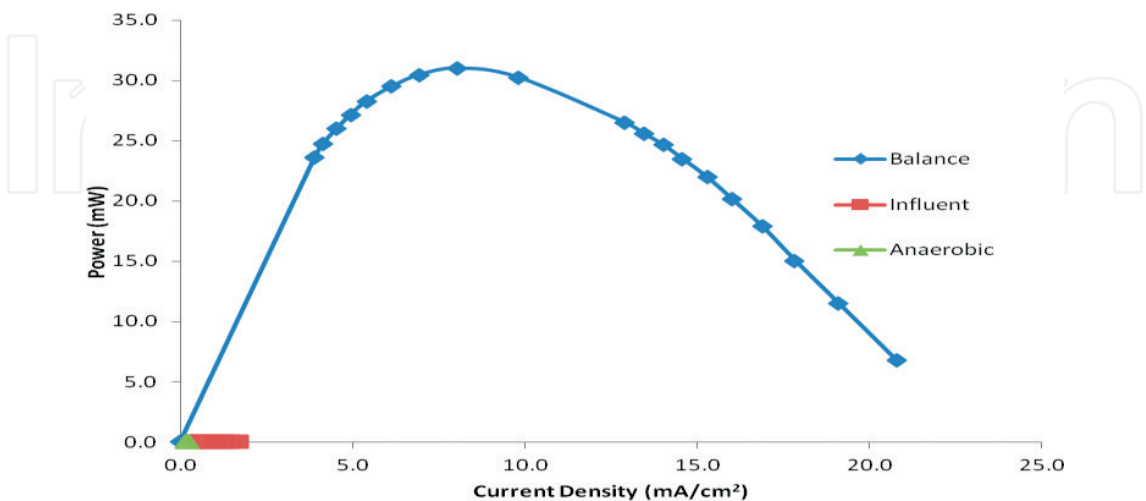

Figure 1. Power density curve for three different wastewaters from same source, but three different treatment methods.
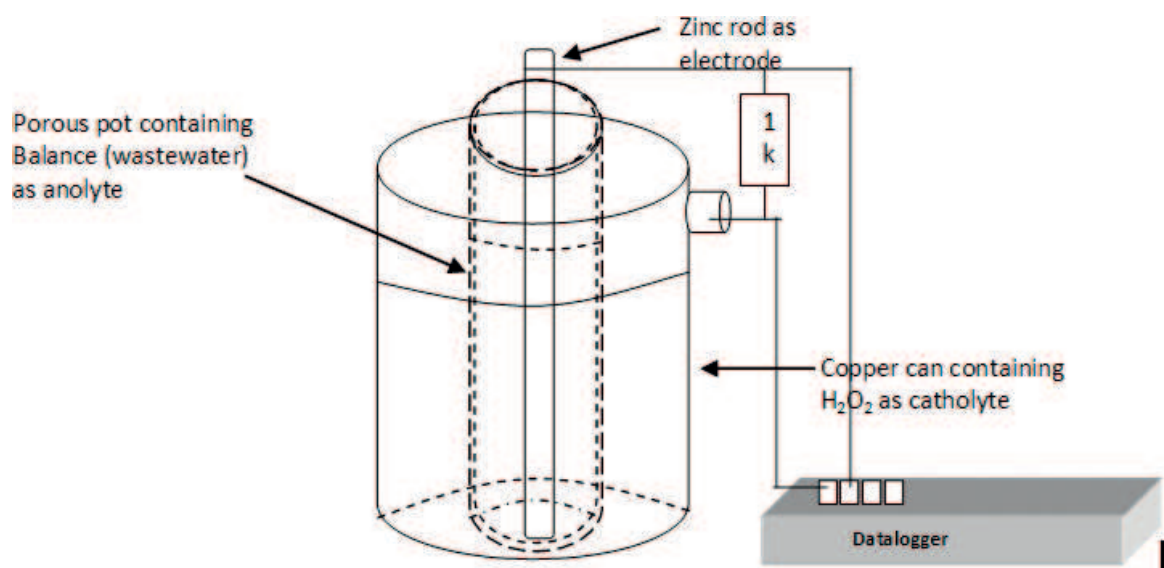
Figure 2. Simplified schematic diagram of double-chamber MFC with porous pot as anode chamber inserted into copper can as cathode chamber. Porous pot is cationic exchange membrane.

the anode and cathode chambers were 5.9 and 6.8 respectively. The setup was then connected to a Datalogger (Campbell Scientific Datalogger CR10X) to store potential difference across the load at 1 min interval. The cell was place in the laboratory condition of ambient temperature between 26 and 29°C and at 1 atm.

3.4.2.2. Results

Table 4 was experimental calculations in terms of current densities and power densities for comparing the normalization. According to Ref. [10] the above parameters sufficiently describe how efficiently a power is generated by a given system architecture. It can be assumed that protons generated from the bacteria metabolism are conducted through the porous pot to balance the charge in the cathode compartment. In this regard, the operation surface area of the pot may have favor anion-cation coupling and thus accounts for the high OCV observed.

3.4.3. Membrane less microbial fuel cell

3.4.3.1. Materials and methodology

Kaolin and Zeolite were used for the ion exchange media in the earlier experiments which were in the process of publication. In this project we designed two pots or chambers which were custom-made cylinders using Mfensi clay. The capacities of the pots are 1.7 and

	Surface area of rod	Inner surface area of pot	Volume of anode substrate
	38.8 cm²	219.44 cm²	300 mL
Max. current density	311 mA/m²	55 mA/m²	4020 mA/m³
Max. power density	375 mW/m²	6628 mW/m²	4848 mW/m³

Table 4. Densities as normalized by the measured parameters.

1 L. Mfensi clay is commonly used in Ghana for drinking water pots. Its porosity ranging from 5 to 25% satisfies a process that cools the content by seeping and evaporation system. That is, part of the content water soaks the pot to the outer part; the outer part then dries gradually extracting the heat from the inner content. The result is that the inner content becomes cooler than the surrounding depending on the rate of evaporation/drying of the outer part. Mfensi clay is also known to have negative charges. The thickness is 1.0 cm and the apparent porosity as measured is 14.3%. We feel these parameters passed for ion exchange to take place. The cells were fed with 1.40 and 0.80 L wastewater respectively from GGBL (Kumasi, Ghana), with initial COD of 4385 mg/L in the anode pots and 40% H_2O_2 surrounding the pots.

3.4.3.2. Results

There are two aspects this experiment sort to compare; 1) to check whether this type of clay can exchange ions and serves as anodic pot; 2) to verify if the size of pot (or operation surface area) affects the amount of power produced.

3.4.3.3. Effect of pot size

As observed through the polarization measurements, the smaller pot performed better as shown in **Figures 3** and **4**, (Pot 1—1.7 L, Pot 2—1.0 L).

Pot 2 yielded a higher potential difference than the pot 1(which contained more substrate in terms of volume). Same applied to the power densities where the peak occurred at 6429 and 4750 mW/m^2 respectively.

As shown in **Figure 5** the polarization curves depict the activation region and the ohmic region (actual performance region), but the concentration region not that clear.
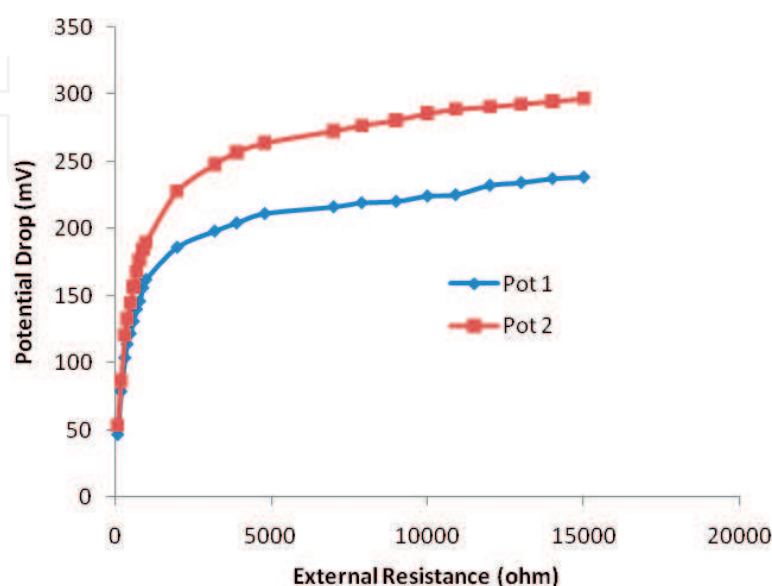

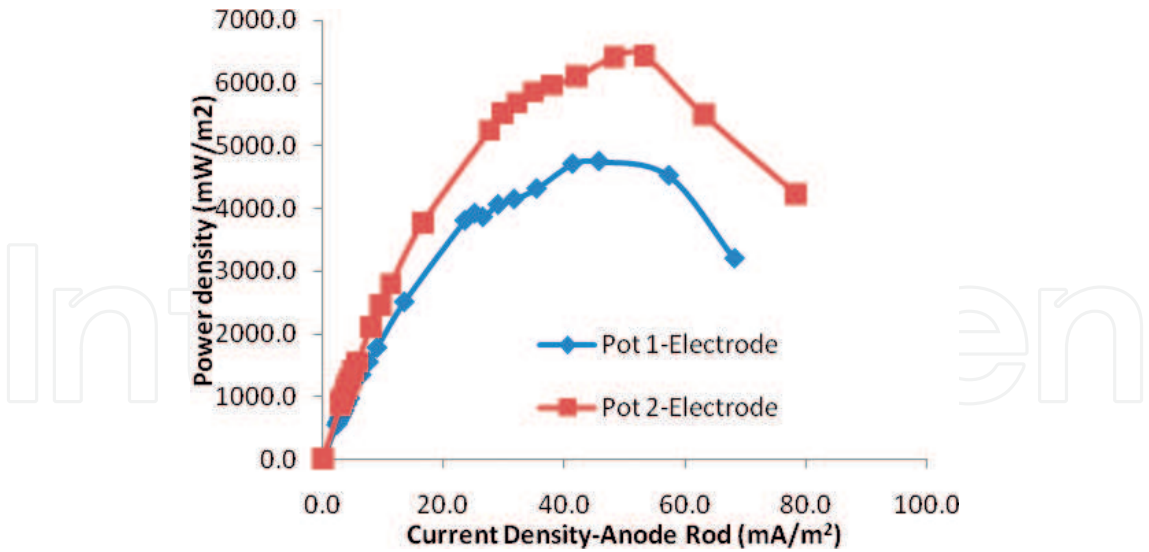**Figure 3.** Variation of potential drop with external load.

Figure 4. Variation of power density with current density as normalized with the anode graphite electrode (same sizes in both cells).

3.4.4. Determination of internal resistance of an MFC

In **Figure 5** the peaks occurred at 0.828 mW/m^2 and 1.53 mW/m^2 for pot 1 and 2 respectively. These values correspond to 330 Ω internal resistance; same for both cells having similar substrate and similar graphite electrodes. The higher OCV value confirms that an MFC that is connected with an external resistance comparable to its internal resistance will produce maximum power [9, 11].
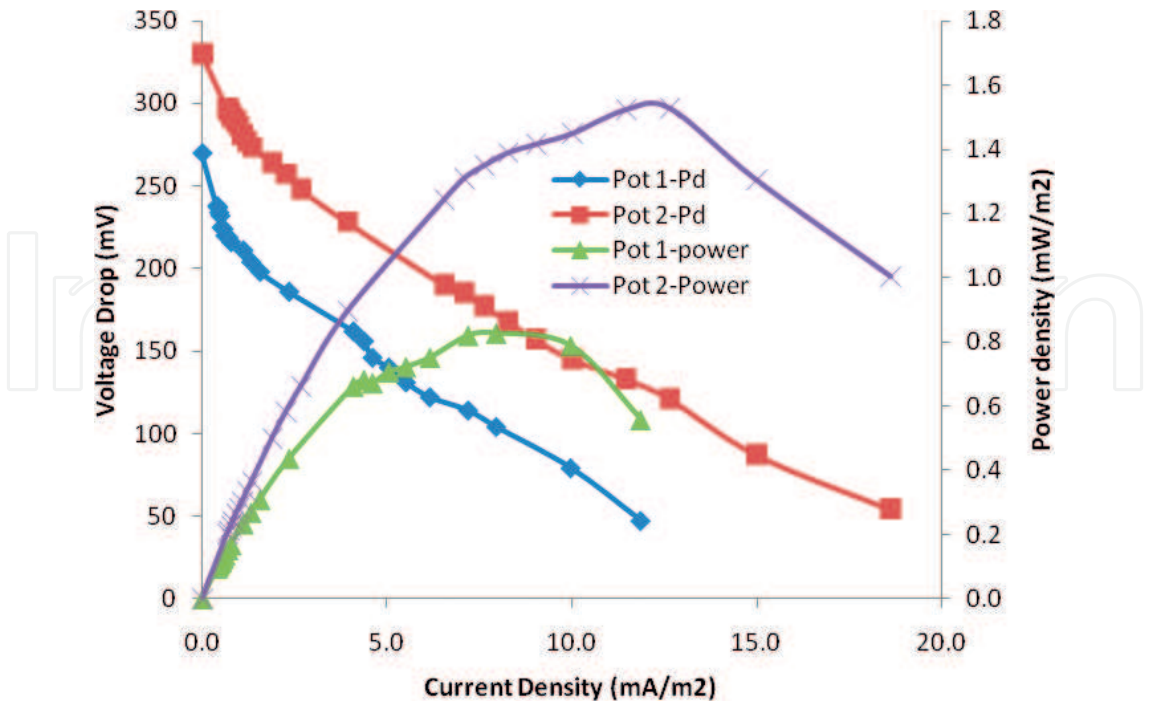

Figure 5. The plotted voltage drop versus current density and power density versus current density curves; normalized with pot operating surface area.

3.4.4.1. Zeolite cells

20% Zeolite was added to Koalin (80%) and molded to a slab of 8 × 8 × 1 cm. This was then fired at the temperature of 3000°C.

3.4.4.2. Results

All the cells were connected to a Datalogger (CR10X) and were observed for 30 days. The open circuit voltage (OCV) for all the cells were recorded every minute and stored for few minutes. Data were then collected via computer interface. **Table 5** shows sample data as collected in excel format.

			Time	Pot 1	Pot 2	Pot—Cu	Pot—Tin	Zeolite
ID	Yr	ProgReg	24 h	OCV/mV	OCV/mV	OCV/mV	OCV/mV	OCV/mV
101	2014	73	1004	−252.7	−123.2	1337.0	980.0	−17.0
101	2014	73	1005	−220.7	−123.2	1337.0	979.0	−12.4
101	2014	73	1006	−179.3	−122.5	1336.0	980.0	−14.4
101	2014	73	1007	−195.3	−122.5	1335.0	1006.0	−19.0
101	2014	73	1008	−202.0	−123.2	1334.0	1024.0	−23.7
101	2014	73	1009	−204.6	−122.5	1335.0	1023.0	−29.0
101	2014	73	1010	−207.3	−123.2	1335.0	1030.0	−32.4
101	2014	73	1011	−210.7	−123.9	1333.0	1029.0	−29.0
101	2014	73	1012	−206.6	−123.9	1331.0	1028.0	−29.0
101	2014	73	1013	−205.3	−118.5	1330.0	1027.0	−31.1
101	2014	73	1014	−206.6	−119.2	1328.0	1025.0	−33.1
101	2014	73	1015	−205.3	−118.5	1326.0	1024.0	−35.1
101	2014	73	1016	−201.3	−117.8	1324.0	1024.0	−35.1
101	2014	73	1017	−196.6	−117.2	1323.0	1025.0	−27.4
101	2014	73	1018	−194.6	−117.2	1322.0	1024.0	−26.4
101	2014	73	1019	−197.3	−116.5	1321.0	1023.0	−26.4
101	2014	73	1020	−193.3	−115.8	1320.0	1023.0	−27.7
101	2014	73	1021	−194.0	−115.2	1320.0	1023.0	−28.7
101	2014	73	1022	−196.0	−115.2	1319.0	1022.0	−29.7
101	2014	73	1023	−194.6	−113.2	1319.0	1023.0	−30.4

Table 5. Sample data as stored by the Datalogger.

Both cells were fed with same wastewater of COD = 4385 mg/L and same diluted H_2O_2. It was found that the OCVs generated by the Cu-Can/porous-pot cell was higher as compared with the zeolite cell, i.e., 1337 and −17 mV respectively. We suspected the zeolite by its property absorbs the ions and release when it can no longer contain it and thus accounts for the negative OCV from the start. Load of 100 Ω was then connected across the terminals of the zeolite cell and 1000 Ω was connected across the pot cell. The recorded voltages now become the potential drop for both DC-MFCs. The readings per minutes were averaged to hours of reading so as to reduce volume of data that can be handled. The result is plotted in **Figure 6**.

It was observed that at the stationary phase microbial growth rate is balanced by microbial death rate as a result of paucity of food and nutrients, as well as the presence of waste metabolic products. Consequently, a stationary population is achieved, but too early or may be due to the flow of current across the bridge. Death phase stage sees to a greater increase in death rate, as compared to growth rate, resulting in a sharp decrease in the number of microbes over the days.

3.4.5. Polarizations

For similar characterization, each cell was subjected to variable loads ranging from 100 to 15,000 Ω and the voltage drop values recorded as given in **Table 6**. This is required to examine the extent to which the cells could be used to power the devices. Both cells were normalized by their operational surface areas; for porous pot the total surface area containing the anodic substrate was 219.4 cm^2 and that for zeolite slab was 16.0 cm^2 (**Figure 7**).
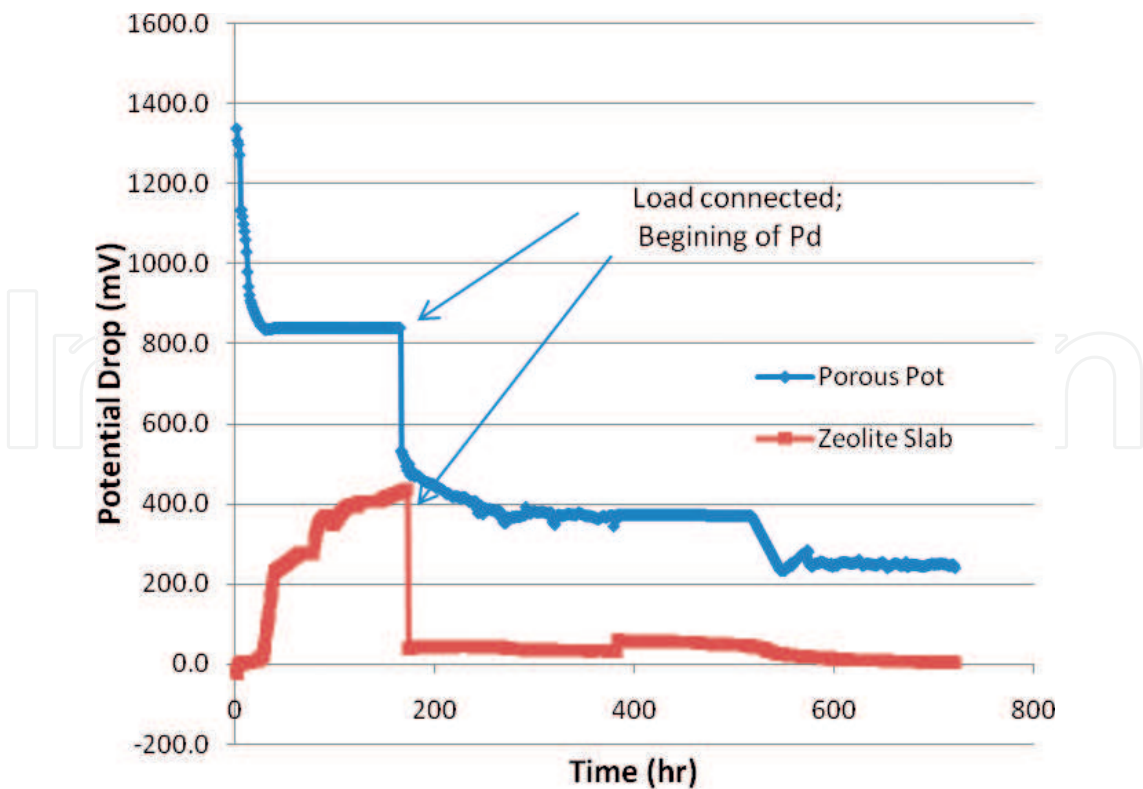

Figure 6. Zeolite and porous pot MFCs: OCV and Pd time variation curves.

	Pot3-Cu: Op-Sf Area = 219.4 cm²				Zeolite: Op-Sf Area = 16.0 cm²			
Resistance	Current	Cur-Den	Pd	Pow-Den	Current	Cur-Den	Pd	Pow-Den
Ohms	mA	mA/m²	mV	mW/m²	mA	mA/m²	mV	W/m²
100	1.610	73.38	161	11.81	0.230	143.75	23	3.31
200	1.425	64.95	285	18.51	0.205	128.13	41	5.25
330	1.155	52.62	381	20.05	0.191	119.32	63	7.52
400	1.060	48.31	424	20.48	0.180	112.50	72	8.10
500	0.934	42.57	467	19.88	0.168	105.00	84	8.82
600	0.842	38.36	505	19.37	0.155	96.88	93	9.01
700	0.774	35.29	542	19.13	0.147	91.96	103	9.47
800	0.710	32.36	568	18.38	0.139	86.72	111	9.63
900	0.660	30.08	594	17.87	0.131	81.94	118	9.67
1000	0.614	27.99	614	17.18	0.124	77.50	124	9.61
2000	0.356	16.23	712	11.55	0.082	51.25	164	8.41
3200	0.235	10.73	753	8.08	0.058	36.33	186	6.76
3900	0.198	9.01	771	6.95	0.050	31.09	194	6.03
4800	0.164	7.47	787	5.88	0.042	26.17	201	5.26
7000	0.115	5.24	805	4.22	0.030	18.84	211	3.98
7900	0.103	4.69	813	3.81	0.027	17.01	215	3.66
9000	0.091	4.15	820	3.41	0.024	15.14	218	3.30
10,000	0.083	3.76	826	3.11	0.022	13.75	220	3.03
10,900	0.076	3.47	831	2.89	0.020	12.79	223	2.85
12,000	0.070	3.17	835	2.65	0.019	11.72	225	2.64
13,000	0.065	2.95	840	2.47	0.017	10.87	226	2.46
14,000	0.060	2.74	843	2.31	0.016	10.18	228	2.32
15,000	0.056	2.57	846	2.17	0.015	9.54	229	2.19

Table 6. Cells characterization data.

It has been found that the *Balance wastewater* produced power most significantly than the other two. It has been observed that the current generation of the cells increased for a higher COD and lower pH. The removal of COD of observed to be highest for the cell which produces higher current. The COD for Balance dropped from 4386 to 267 mg/L for the 36 days of running (**Tables 7** and **8**). Summary of other Generated Parameters:
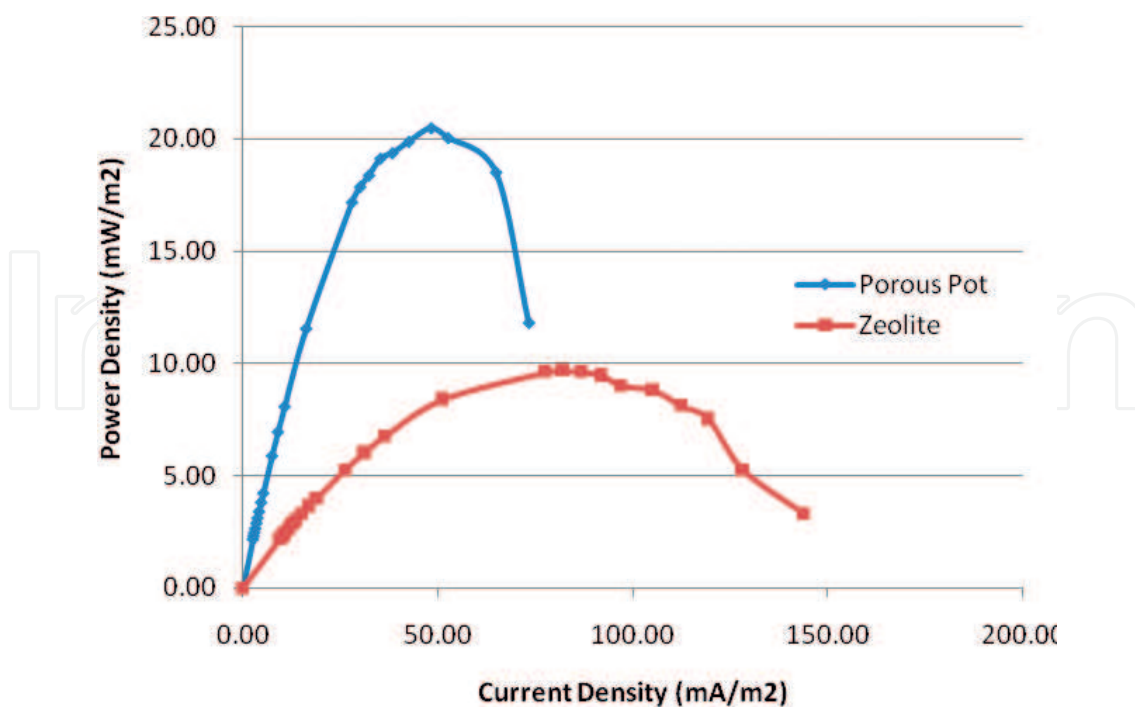
Figure 7. Polarization power curves for kaolin/bentonite porous pot and clay/zeolite pot.

Substrate	Max. OCV (mV)	Max Current (mA)	Power Density (mW/cm²)	Current Density (mA/cm²)	Internal Resistance (Ω)
Balance	782	0.330	246	8.04	3 k
Influent	345	0.021	37.9	0.34	8 k
Anaerobic	66	0.003	10.7	0.028	10 k

Table 7. Observed results in relation with types of wastewater.

Parameters	Pot 1	Pot 2
Initial COD	4385 mg/L	4385 mg/L
Final COD	571 mg/L	522 mg/L
% COD removal	86.98	88.10
Apparent porosity	14.3%	14.3%
OCV (mA)	300	250
R_{int} (Ω)	330	330
Imax (mA/m²)	11.87	18.62
Pmax (mW/m²)	4750	6429

Table 8. Measured MFCs characteristics of the two pots.

The factors that affect the cathode and anode potentials were investigated. Compared with other membrane types, cation exchange partition, clay anodic container and aluminum cathode container assembly yielded such performance. This system might be useful in applications of MFC type at a very low cost. Mfensi clay is said to have negative charges which might be responsible for negative OCV. This approach represents a potential solution for simultaneous electricity production and removal of COD and thus offers a technological tool both for sustainable energy generation and for economic viability.

Both, double chamber membrane-less-microbial-fuel-cells (MLMFCs) were found to give COD reduction greater than 88%, with maximum power production 20.48 mW/m^2 as normalized with the anodic substrate container surface area. It was expected to generate enough power to light a LED through only one cell so as to be able to power low voltage circuits or devices. However, efforts are being made to improve the structures of Zeolite DC-MFC for better performance.

4. Section B

4.1. Effect of COD and H_2O_2 concentration on double chamber MFC (DC-MFC)

In the present section an attempt has been made to investigate the effect of hydrogen peroxide (H_2O_2) and COD on the performance of DC-MFCs. It has been found that 80% H_2O_2 or a mixture of 1:4 exhibited higher power generation while 20–60% concentration have no effect. This shows that H_2O_2 can be used as oxidizing agent between the concentrations of 70–90%. The values of power densities of the order 24.56 W/m^2 for Balance substrate (7562 mg/L COD) for 80% H_2O_2 confirms the effect of CODs on the performance of DC-MFC.

The results of this study indicate that the efficiency in DC-MFCs can effectively be increased by varying the concentration of H_2O_2 as cathodic substance. Specifically, the investigation shows that this paper supports the earlier result by [9] of the use of hydrogen peroxide as cathode substrate. Upon investigation of different catholyte concentrations, dilution of H_2O_2 at a certain level must be necessary to achieve high efficiency and power generation.

4.2. Fabrication of DC-MFC

The MFC chambers were fabricated using plastic containers of two equal volume of 1.8 L each. These anode and cathode chambers were separated by proton exchange membrane (PEM—Nafion 117) [9] as shown in **Figure 8**.

Two different kinds of waste water obtained from the Guinness Ghana Brewery Limited (GGBL—Kumasi) were used in the anode chambers, one with COD—1273 mg/L and the other with COD—7562 mg/L. the cathode chambers were filled with H_2O_2 mixed liquid. Plain graphite rods of surface area 86.7 cm^2 were used as cathode and anode; as the surface area of anode does not affect power production [10]. The voltage and current were measured with a Digital multimeter (Peak Tech® 2010 DMM).open circuit voltage E was obtained and stored using a data acquisition system (Campbell Scientific Ltd. Datalogger—CR10X).
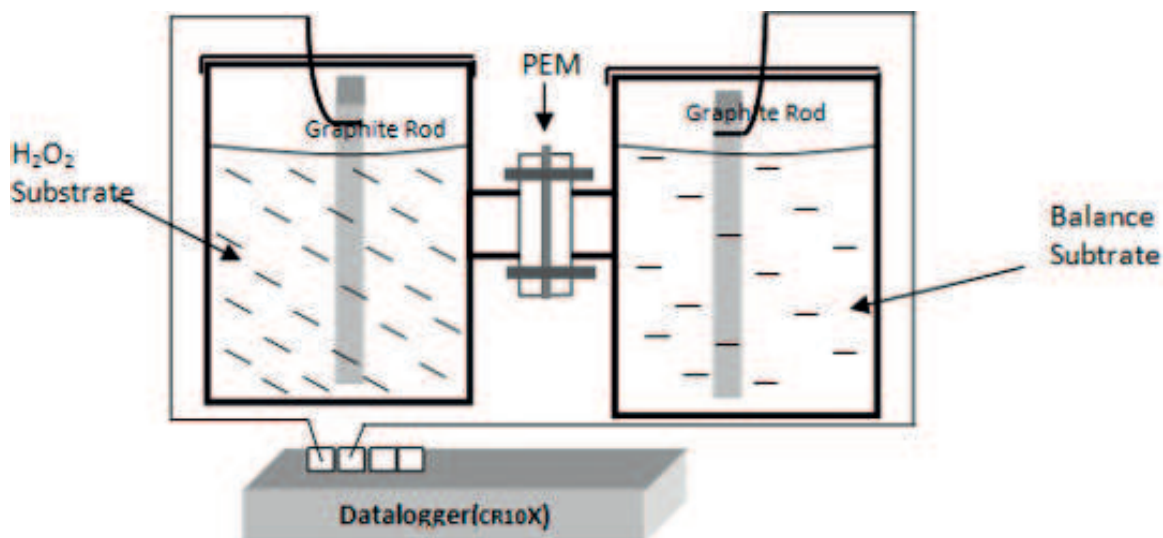
Figure 8. Double chamber PEM setup.

In systems that contain a membrane separating the two electrode chambers, it is possible to normalize power based on the membrane projected surface area;

Current Density normalized by PEM area $= \dfrac{E}{A_{PEM}}$

Power density as normalized with PEM area $= \dfrac{E^2}{R \, x \, A_{PEM}}$

Power density as normalized with volume of anode chamber $= \dfrac{E^2}{R \, x \, V_{an}}$

Where E is load voltage, R is load resistance, A_{PEM} is active PEM area and V_{an} is volume of anode chamber.

4.3. Results

The open circuit voltage as against concentration of H_2O_2 at the anode chamber is shown in **Figure 9**. Whereas the open circuit voltage in relation with time has been shown in **Figure 10**. Also the variation of power with current density for various concentrations of H_2O_2 is shown in **Figure 12**.

The drops and the ramps were observed to occur in the nights where the temperature dropped from 28°C to between 27°C and 25°C. This temperature effect may not be for the peroxide, but for the biological substrate.

Polarization curves were obtained by varying external resistances from 100 to 10,000 Ω (**Figure 11**).

As may be seen in the above **Figure 9**, the 80% concentration at the cathode exhibited a significantly high polarization than expected. It should also be observed that the addition of 20% water showed about 80% increase in voltage over the pure peroxide (100%). The fact that the other concentrations in the cathode chamber performed so poorly in comparison to the 80% concentration is evidence that potential difference may be dependent on the number of ions exchanged between anode and cathode chambers. Non-diluted hydrogen

peroxide (100%) in the experiment washed the surface of the cathode clean. This may be due to the high reactivity of H_2O_2. This also shows that H_2O_2 is an oxidation agent between 75–90% concentration.
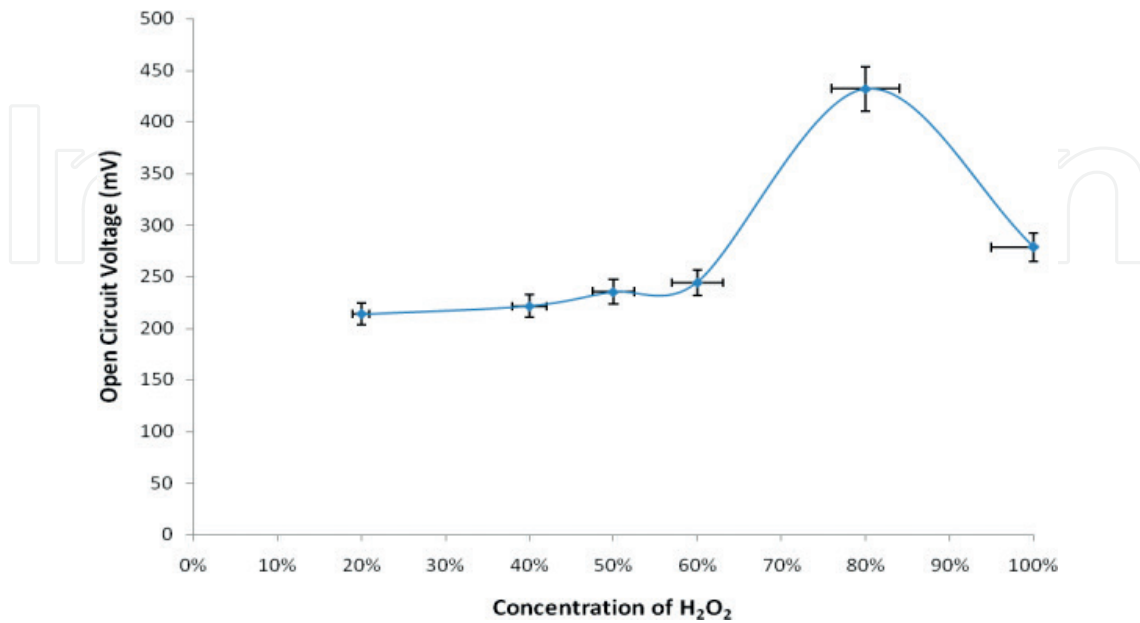

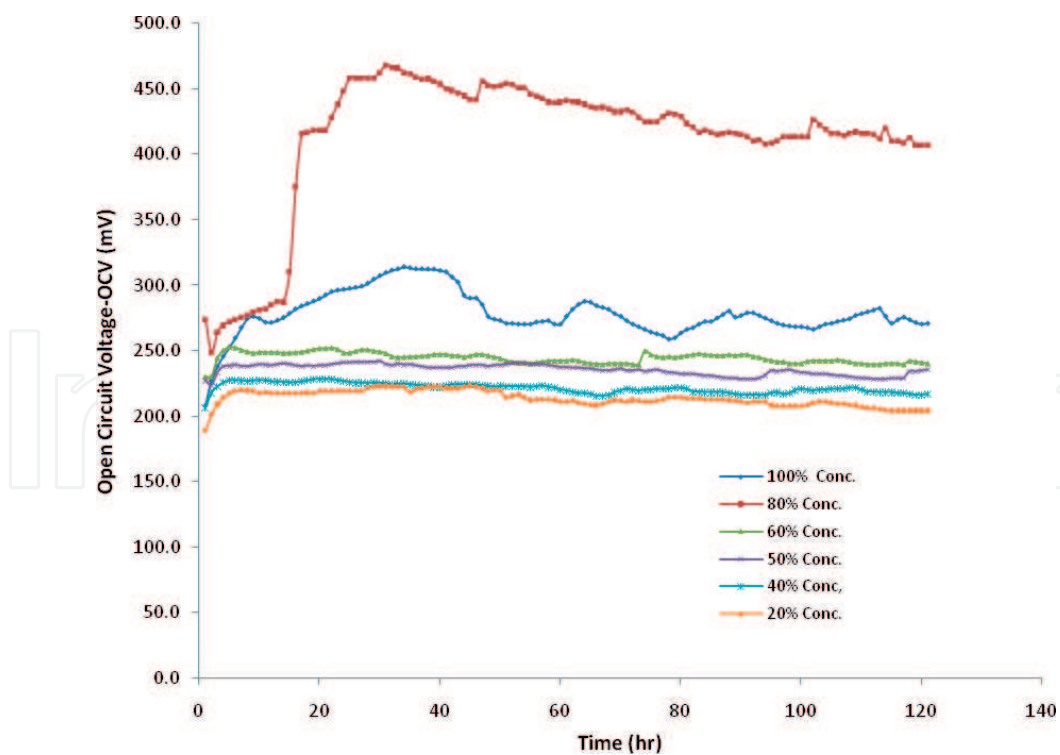**Figure 9.** OCV versus hydrogen peroxide concentration.

Figure 10. Performance comparison in relation to open circuit voltages plotted as a function of time for varying concentration.
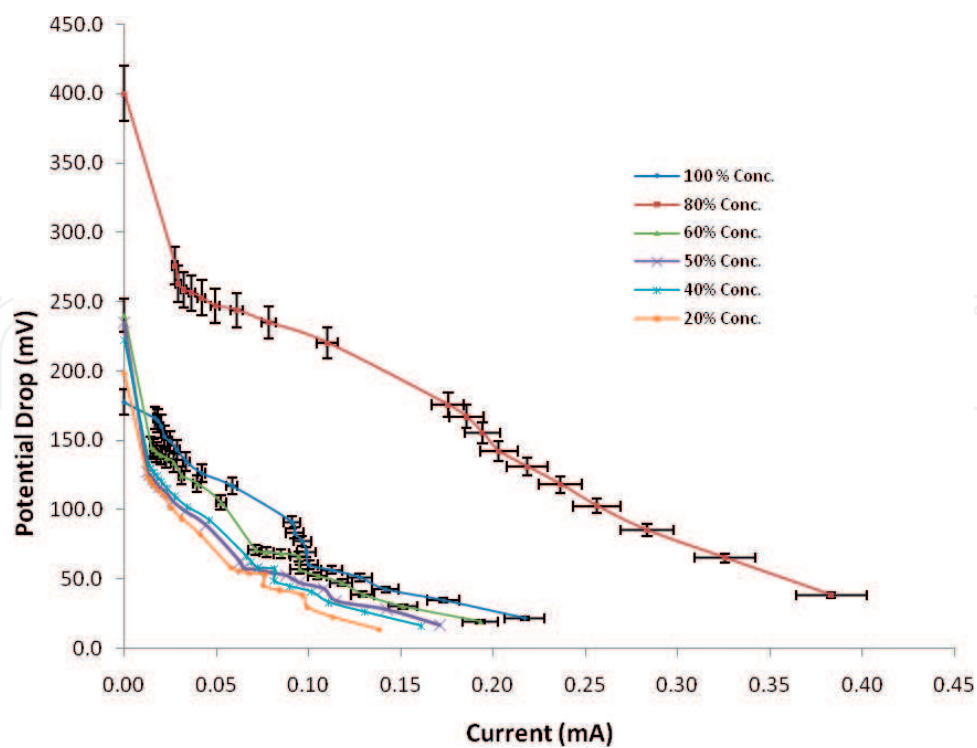
Figure 11. Performance comparison in relation to hydrogen peroxide (6% w/v with stabilizer) concentration.
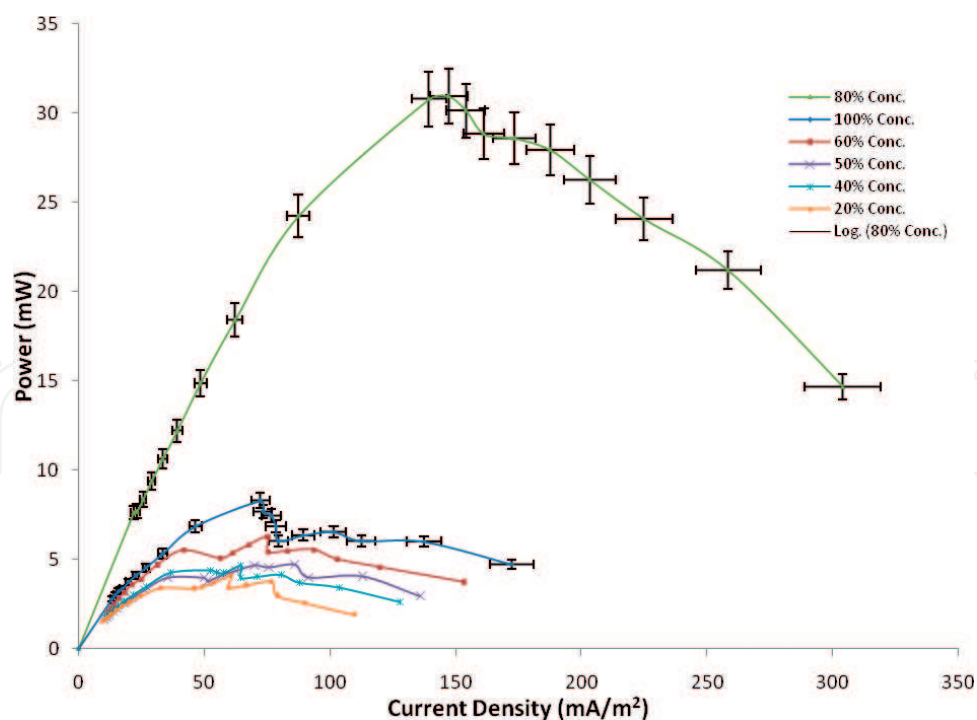
Figure 12. Variation of power with current density for various concentrations of H_2O_2.

Similar characteristics were observed for power versus current density relationship. Maximum power density as normalized with PEM area is 24,564 mW/m², which is equivalent to 17.2 mW/L as normalized by substrate volume.

4.4. Effect of CODs and H_2O_2 concentration on power density

As H_2O_2 concentration is crucial in this experiment as the CODs of the substrates, though the percentage dilution has significant impact on the performance of the two systems. Moderately, the earlier result indicated that the power density actually depends on the COD of the anodic substrate. As shown in **Figure 12** the OCVs were not far apart and thus compare favorably, but this could not be said about their power densities. From 20 h on more ions may have been released as bio-activity increases. The peaks of their power densities were far apart and would have been dependent on the CODs of the two systems as exhibited in **Figure 13**.

The OCV may be similar, but as current strictly depends on the number of useful electric charges present in the system are responsible of bio-electrochemical reaction; the reason would be probable.
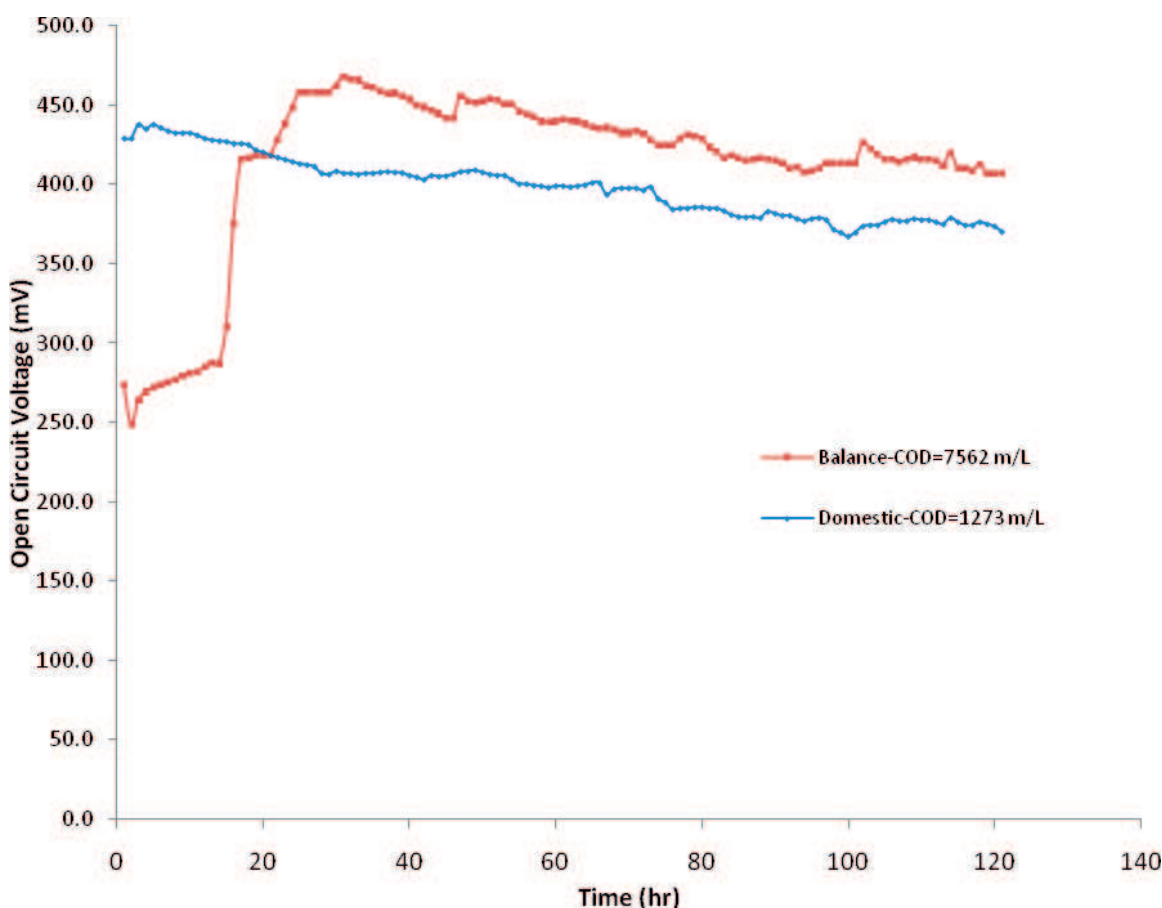
Figure 13. Comparative state of the two similar MFCs.

5. Section C

5.1. Multi-chamber microbial fuel cells (MFCs) with clay as ion exchange partition

This section includes the performance of multi-chambered MFCs. Performance of each micro cell in the system was observed to be significant in terms of their yields as could be in standalone single cell. Each adjacent cell tends to supplement the other so that series configuration is not possible in the same multi-system. In parallel configuration, all anode terminals connected as one and all cathode terminals connected together, resulting in higher current as shown in **Figure 14**. This higher power can therefore perform for longer period when connected to a load. Few experimental uses attested to such performances.

5.1.1. Materials and methodology

The clay material was obtained from Mfensi, a town near Kumasi—Ghana. As in **Table 9** was the constituent of the clay as used in the earth wares sold in the market.

The varying chambers were molded and fired at the Department of Ceramics, KNUST. The chambers were in 2, 4, 6, and 9 sets. As in **Figure 14** a chamber is 3.8 × 3.8 × 9 cm (approx. 130 cm^3 in volume) and 0.6 cm thick. Porosity was measured to be 14%. The outer part of each set of pot was coated to prevent the liquid seeping out.

5.1.2. Wastewater used in MFCs

Wastewater from the Guinness Ghana Brewery Limited (GGBL, Kumasi) has being our favorite for anode substrate, primarily because of its known source and safety measures attached to its disposal. Besides, it is suitable for electricity generation in MFCs due to the food-derived nature of the organic matter. Good results were obtained in earlier studies with this wastewa-

Element	%	Element	%
Na_2O	6.15	K_2O	1.66
MgO	1.28	CaO	0.54
Al_2O_3	13.82	TiO_2	0.04
SiO_2	65.26	MnO	0.07
P_2O_5	0.23	FeO_3	0.83
SO_3	0.10	LOI	10.00
Cl	0.02	**Total**	**100**

Table 9. Composition of Mfensi clay from geological survey department (Ghana) X-ray fluorescence laboratory results.
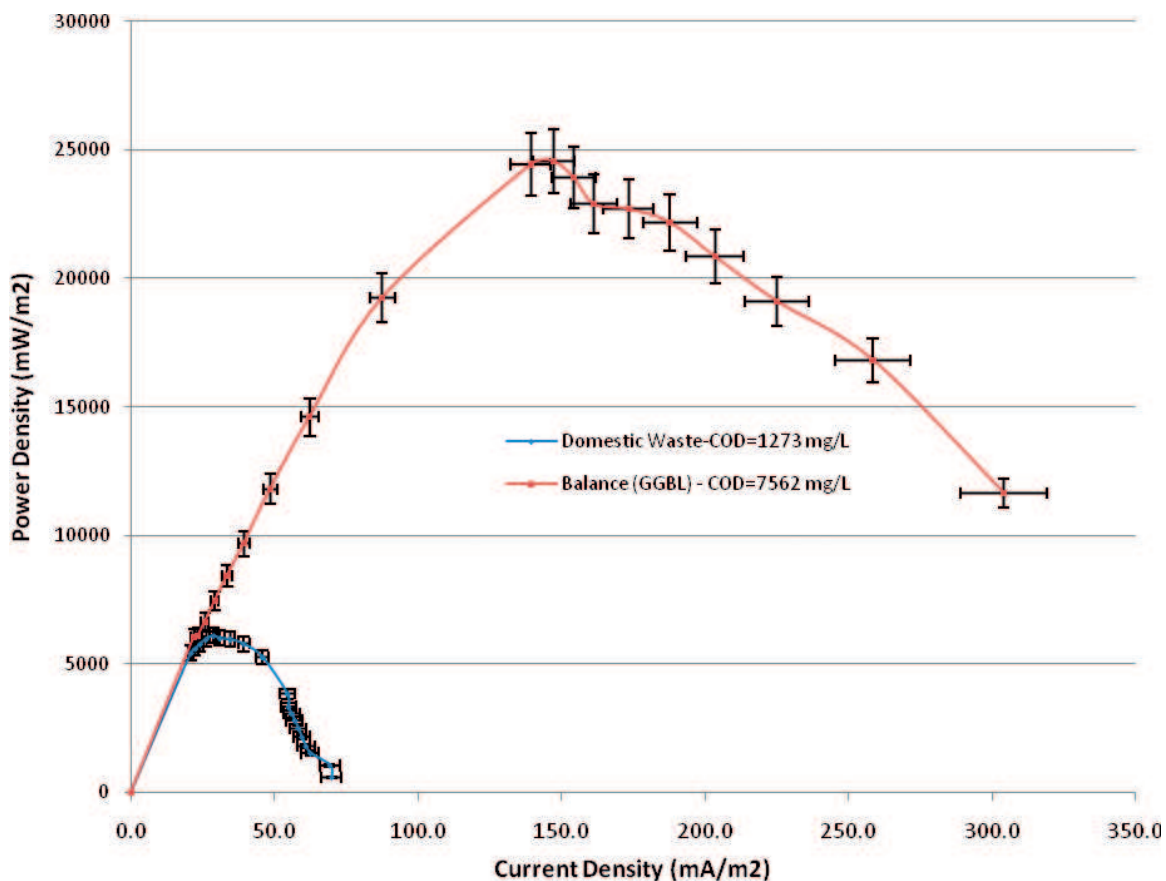
Figure 14. Comparative power densities versus current densities of the two MFCs.

ter with varying CODs [9, 12, 13]. Each cell was fed with wastewater of COD equals to 6340 gm/L and 80% concentration of H_2O_2 alternatively. 80% concentrated H_2O_2 was done earlier to ascertain the veracity of suitable dilution for higher performance [13].

5.1.3. Choice of electrodes

Most of the publications on suitable electrodes [10, 14] have laid emphasis on carbon and its variance, but these experiments continually use zinc rods and copper plates for good results. In the present work, zinc plates of surface area 24 cm^2 each were inserted in the wastewater and copper rod of same surface area placed in the H_2O_2 respectively making each adjacent pot forming a cell (**Figure 15**).
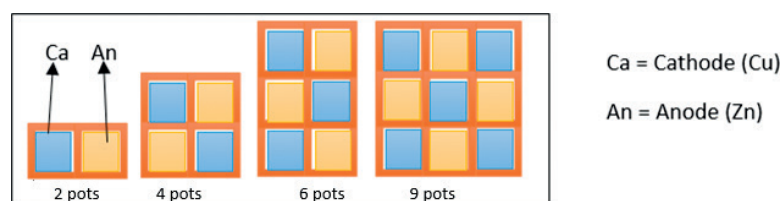
Figure 15. Designed and fabricated Mfensi clay chambers; anode/cathode chamber applied to all cells.

5.1.4. Measurements

Each cell was connected to Datalogger (Campbell Sci CR10X), open circuit voltage (OCV) and potential drop across 1 K load were recorded per minute for 35 days. Ambient temperature varied over the period between 24°C and 25°C.

5.2. Parallel connection

4, 6 and 9 combinations were connected in parallel (**Figure 16**) and to the Datalogger. That is, zinc plates in each anode pot were connected together and copper plates were also connected together as one terminal.

5.3. Series connection

Series connection in the multi system appeared isolated and as in **Figure 16b** each cell was connected to a load and thus tend worked independently. Such single cell measurement was plotted in **Figures 17** and **18**.

5.3.1. Results

There were two aspects of these experiments sort to compare; 1) measure the performance of single cell in the multi MFC system; 2) performance of total multi cell as a single cell. Although all the cells were co-joint with each other as the partition between them act as ion-exchange medium. Each adjacent pot combination in the alternative forms a cell. The cells were also taken through the polarization measurements using resistors of 100–15,000 Ω. Voltage drops were recorded through PeakTech 2010DMM Multimeter.

First portion of **Figure 17** (A) on the curves presented OCVs recorded by the Datalogger without load. When the loads were connected there were sharp drops in line with ohm's law of electric circuit calculation [15]. Some of the cells continually dip with hours of operation while others maintain constant voltages (B). 9 and 6 chambered cells configured into parallel cells each respectively, were the top 2 of higher operation voltages, meaning these can be used for longer operation period.
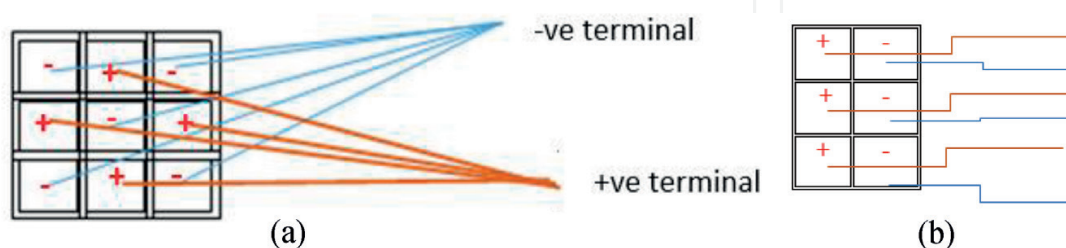

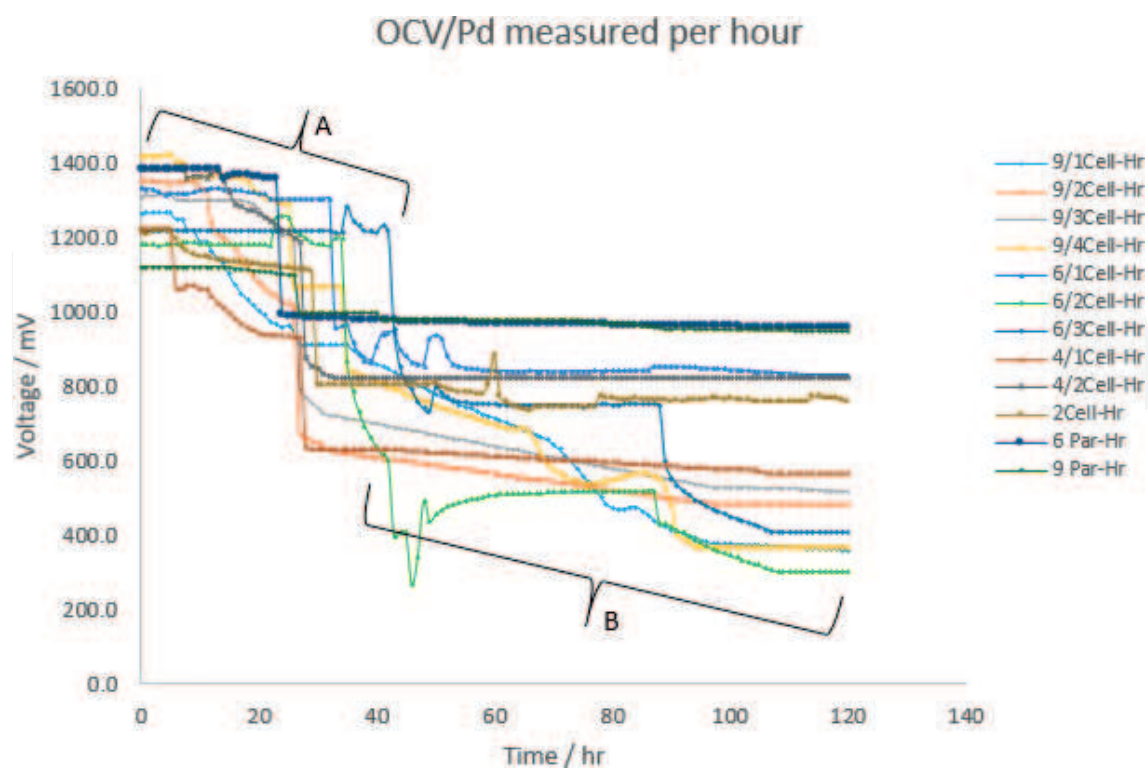**Figure 16.** (a) Parallel cell configuration (9 chambered cell); (b): Series cell configuration.

Figure 17. Voltage recorded for the first 5 days.
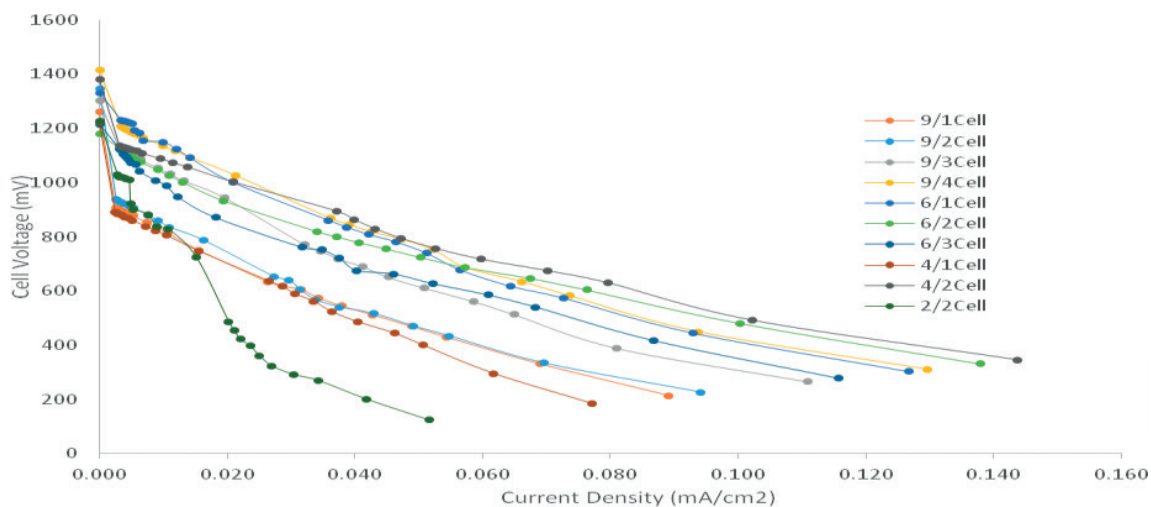

Figure 18. Voltage drop across varying resistors against current density.

Current density was calculated based on the surface area of the anode electrode ($I_D = Pd/RA_{an}$), and Power density was then calculated using $P = I_D E$ (where I_D is the current density and E the voltage drop).

It was observed that OCV did not follow a pattern (**Figure 18**). The fourth cell from the 9 chambered cell had the highest OCV of 1414 mV which was probably due to the fact that this particular cell had two anodes and one cathode.

From both polarization and power curves for 4/2Cell show the highest yield, compared to 4/1Cell. Although the OCV for 9/4Cell was highest it was not consistent with ohmic portion of characteristic curves of **Figures 18** and **19**. These curves show how well the cells maintain voltages as a function of the current produced. Resistive effects in fuel cells reduce the
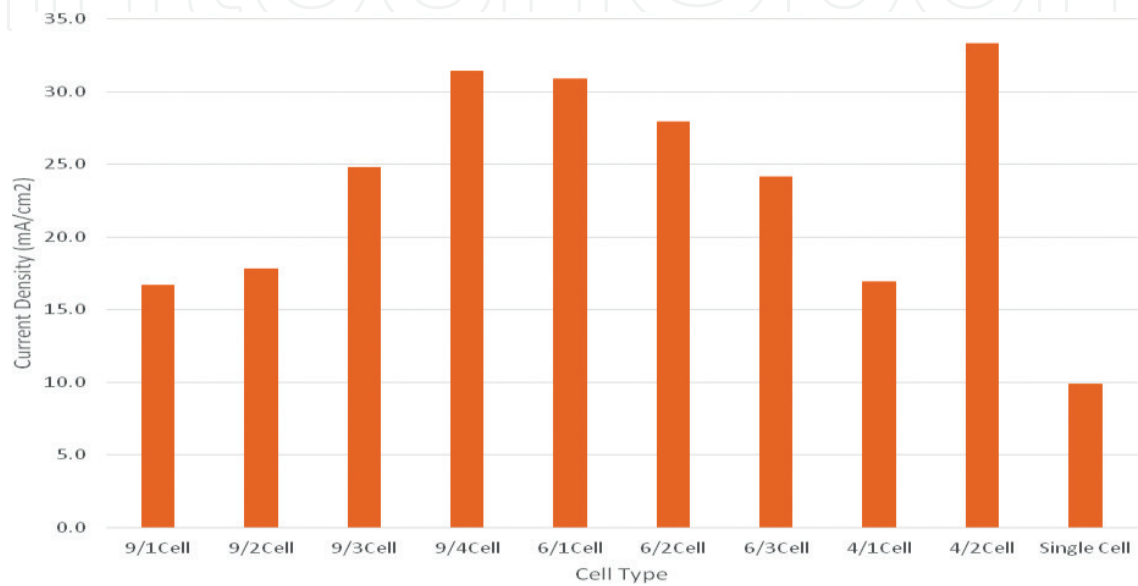
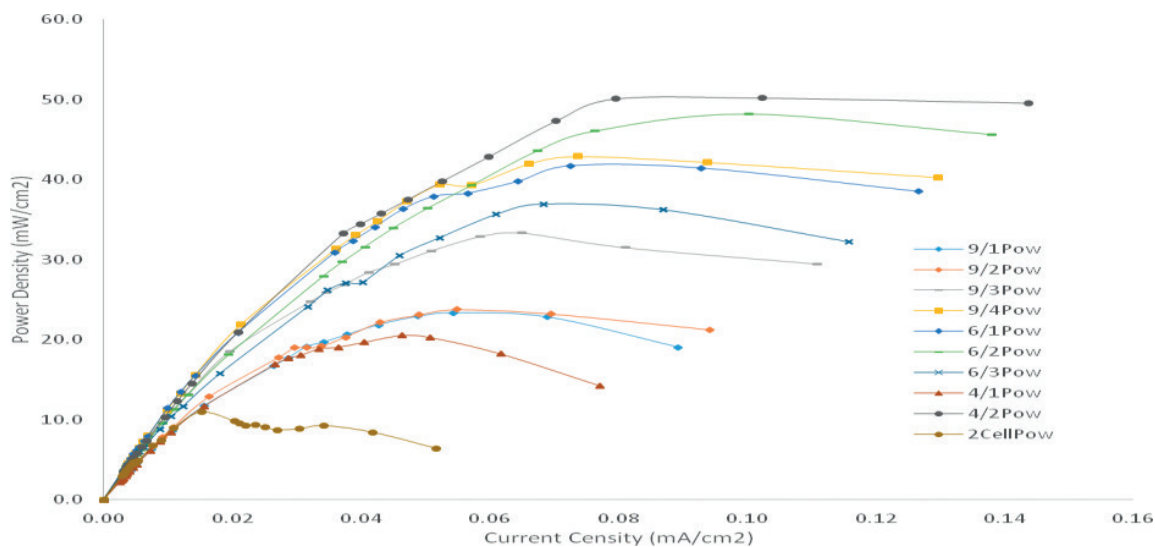**Figure 19.** Histogram resulting from **Table 10**.

Figure 20. Power density verse current density comparing individual cell in multi MFC system.

efficiency of the cell by dispelling power in the partitions and substrate resistances. This effect is also observed due to the insulation of the anode electrode. The voltage generated here is far more complicated to understand or predict, and as usual the inference can be deduced from the total result. Almost all the individual cells have their internal resistance R_{int} = 330 Ω, and [10, 15, 16] we see that the maximum power resulted at a point where $R_{int} = R_{ext}$, then $P_{max} = E_{emf} /4R_{int}$ [17].

The parameter that must have caused the variation in nature of the histogram with regards to 4/2Cell might be due to the partition characteristic between anode/cathode of the cell, with all other factors been the same; i.e. substrates, anode, cathode and ambient conditions.

The maximum power as shown in **Figure 21** was 41.25 mW/cm^2 for 9 chambered cells. The activation losses and ohmic portions of the polarization curves were more pronounced in both **Figures 17** and **20**. The concentration polarization drops were overcome within the range of load/resistors (100–15,000 Ω) used for the measurements. Concentration losses are most important loss parameters to be overcome for optimum design of the MFC architecture. These losses were said to arise from resistance of ion conduction due to the substrates and the membrane or partition between anode and cathode, the flow of electrons through the electrodes to the contact load points [10]. Our choice of clay partition could have accounted for reduction in concentration losses and also ensuring good contacts in the circuit, and the source of anode substrate that enhanced solution conductivity.
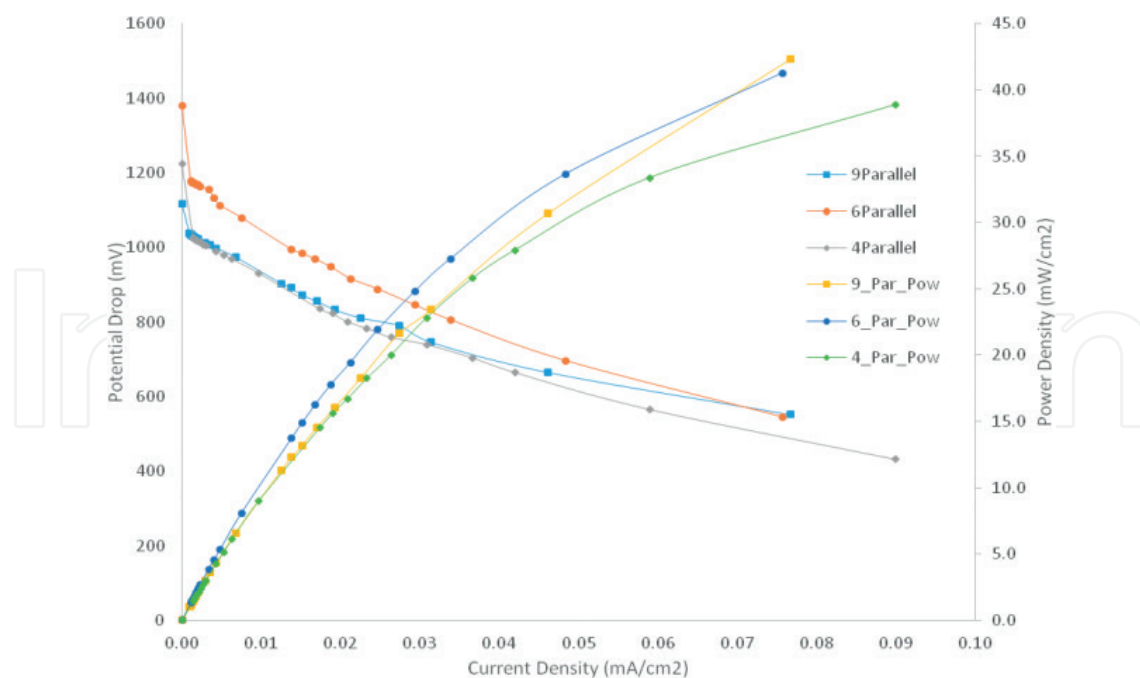

Figure 21. Polarization and power density curves for parallel combination multi MFC system.

	OCV/ mV	Resistance/Ω	Pd: E/ mV	Current/mA	Current Density/mA/ cm²	Power Density/mW/ cm²
9 Chambered cells	1260	1000	633	0.633	0.0264	16.6954
	1347	1000	654	0.654	0.0273	17.8215
	1302	1000	771	0.771	0.0321	24.7684
	1414	1000	868	0.868	0.0362	31.3927
6 Chambered Cell	1331	1000	861	0.861	0.0359	30.8884
	1179	1000	819	0.819	0.0341	27.9484
	1215	1000	761	0.761	0.0317	24.1300
4 Chambered Cell	1223	1000	637	0.637	0.0265	16.9070
	1380	1000	894	0.894	0.0373	33.3015
2 Chambered (one cell)	1228	1000	486	0.486	0.0203	9.8415
9 Parallel (as one cell)	1118	1000	903	0.903	0.0125	11.3251
6 Parallel (as one cell)	1380	1000	994	0.994	0.0138	13.7227
4 Parallel (as one cell)	1223	1000	835	0.835	0.0174	14.5255

Table 10. Comparison of individual cells in the multi MFC system.

6. Section D

6.1. Mfensi clay as ion-exchange-partition in double chamber microbial fuel cells (DC-MFCs)

This section includes the development of a low cost double chambered microbial fuel cells (DC-MFCs) for power generation as well as for wastewater treatment simultaneously. These fuel cells were fabricated using a locally available Mfensi clay as an ion-exchange-partition. These cells also used pot-electrode combination that is: (1) pot-graphite/graphite combination and (2) pot-zinc/copper combination. Both MFCs were connected to a Campbell Datalogger CR10X to measure and store initial open circuit voltages (OCV) as well as potential drops across 1000 Ω resistor for 30 days. Experimental results showed maximum power densities of 118 and 79 mW/m² for the Pot-zinc/copper pair electrode and Pot-graphite/graphite pair electrode respectively.

6.2. Materials and architecture of DC-MFCs

The materials used for this work includes Mfensi clay from the Atwima Nwabiagya District in Ashanti Region of Ghana, The clay is known to have negative charges. Two cylindrical chambers (**Figure 22**) of capacities of 1.7 and 1 L and thickness of 1 cm were fabricated

Figure 22. Pot 1 and 2.

from the clay and fired at a temperature of 1050°C in the Department of Ceramics – College of Arts and Social Sciences, KNUST. The apparent porosity of the cylinders as measured was 14.3%. **Figure 23** shows an MFC assembly consisting of an improvised cathode which was an Aluminum cooking utensil housing the cylindrical chamber and also containing 40% diluted hydrogen peroxide (H_2O_2). The ion-exchange partition houses the anodic substrate. The two cells under investigation were fed with 1.40 and 0.80 L wastewater respectively from Guinness Ghana Breweries Ltd. (GGBL- Kumasi, Ghana), which had an initial COD of 4385 mg/L.

6.3. Results and discussion

Figure 24 shows the variation in potential drop (OCV) with time for zinc/copper and graphite/graphite electrode pairs.

Pot-graphite/graphite pair yielded contrary results although same substrates were used. The results obtained for this electrode pair (the lower curve of the plot) shows a gradual rise of the initial OCV of −300 mV to almost 0 V after which a gradual fall was observed over the time period. The negative result of pot-graphite/graphite pair was thought to be the effect of negatively charged of Mfensi clay that tend to neutralize the incoming positively charged ions from the anode.

The polarization curves as well as plots of power densities versus current densities for cells loaded with incremental load of 100–1500 Ω have been depicted in **Figures 25–27**. **Figure 25** shows that pot-zinc/copper pair produced higher values in relation to the applied external
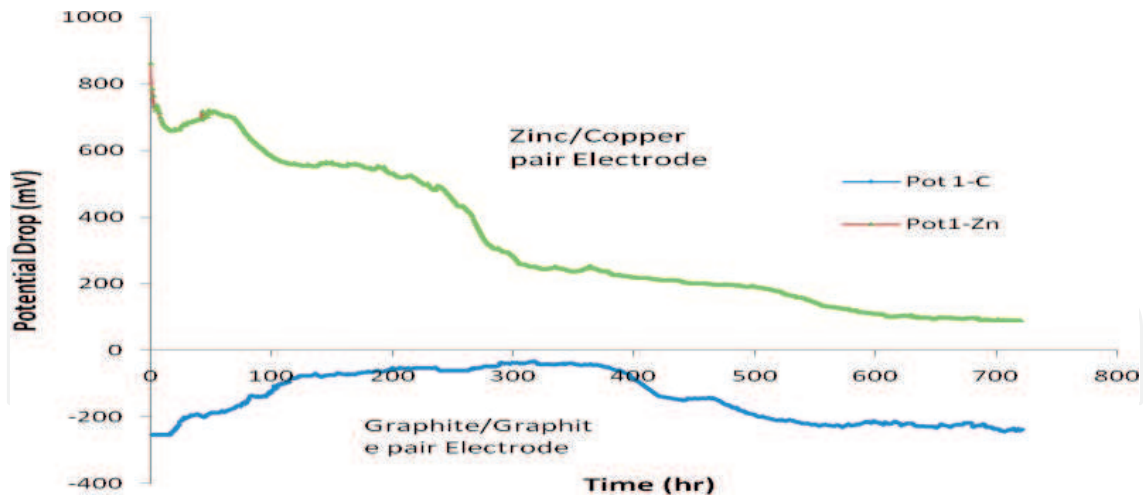

Figure 23. MFC assembly.

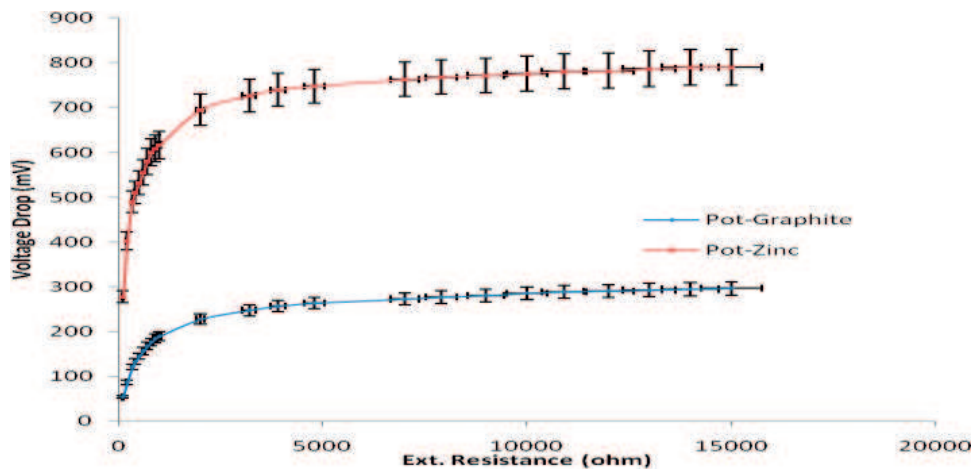**Figure 24.** Variation in potential drop (OCV) with time.

Figure 25. Variation of potential drop with external load relating to pot-graphite/graphite pair and pot-zinc/copper pair.

loads ranging from 0 to 15,000 Ω and **Figure 26** shows the variation of potential drop with current density relating to pot-graphite/graphite pair and pot-zinc/copper pair.

6.4. Determination of internal resistance of the cells

The internal resistance is one of the major characteristics of a MFC, in accordance with the theorem of maximum power delivered by an electromotive force. An MFC connected with an external resistance equals to its internal resistance will give a maximum power output [10, 11]. From **Figure 27** the peaks occurred at 118 and 79 mW/m^2 for zinc/copper and graphite/graphite systems respectively. The alternative to finding internal resistance was calculated from the slope of **Figure 26**. The peak value corresponds to 200 Ω internal
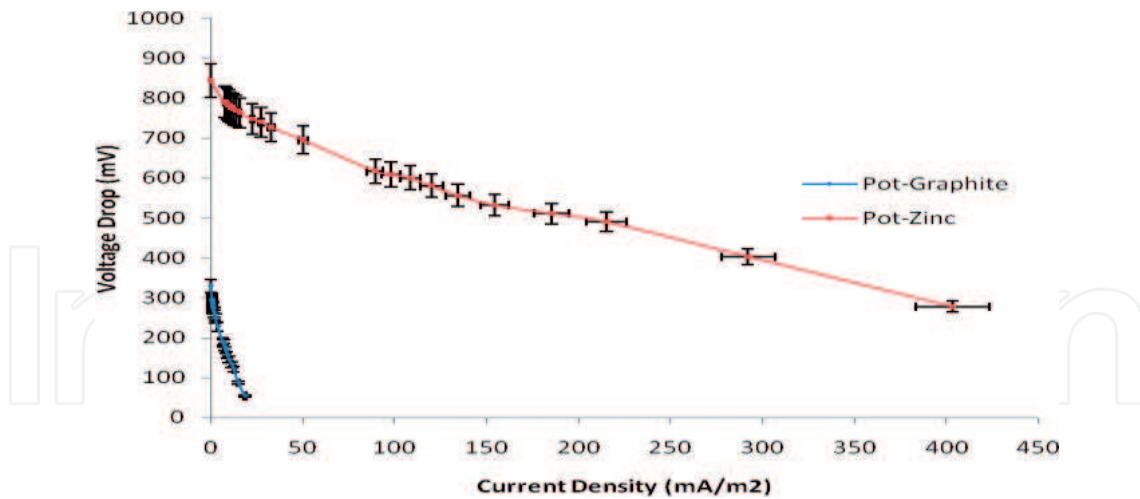
Figure 26. Variation of potential drop with current density relating to pot-graphite/graphite pair and pot-zinc/copper pair.
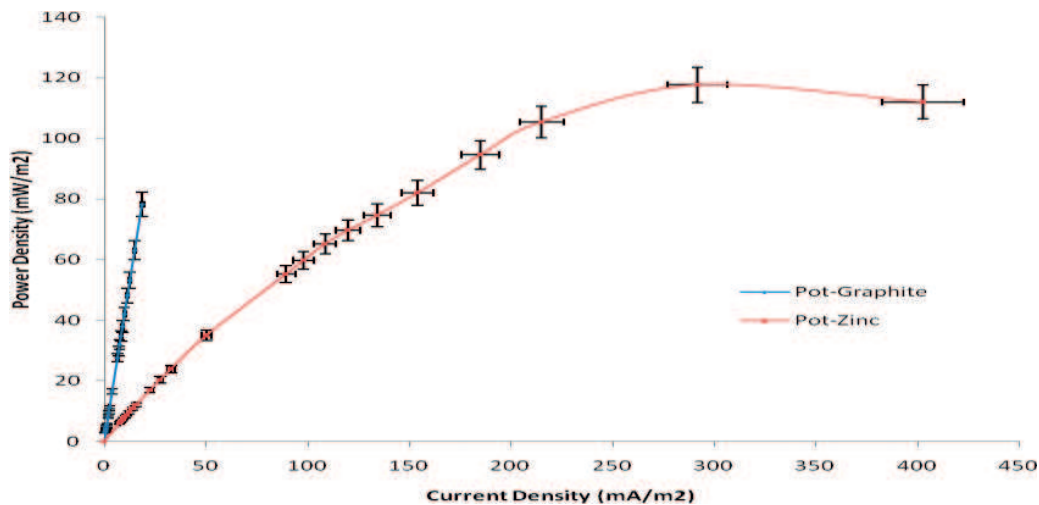

Figure 27. Variation of power density versus current density as normalized with the anode electrodes relating to pot-graphite/graphite pair and pot-zinc/copper pair.

resistance for zinc/copper system and 556 Ω graphite/graphite. The internal resistance however seems to be high for graphite/graphite system, as can be anticipated using the polarization curve method (**Table 11**).

The unconventional inexpensive Mfensi clay ion-exchange medium used for the study seems to be a viable alternative to the conventional expensive PEM. It was observed that a porosity of 14.3% may facilitate the flow of liquid in both directions though. We believe it holds the future for improvements in MFC performance. This approach represents a potential solution for simultaneous electricity production and removal of COD and thus offers a technological tool for sustainable energy generation.

	Pot-Zn/Cu	Pot—C/C
Initial COD	4385 mg/L	4385 mg/L
Final COD	571 mg/L	522 mg/L
% COD removal	86.98	88.10
Apparent porosity	14.3%	14.3%
OCV (mV)	800	−250
R_{int} (Ω)	200	556
I_{max} (mA/m^2)	403	19
P_{max} (mW/m^2)	118	78
Initial pH (H_2O_2)	6.8	6.8
Final pH (H_2O_2)	7.9	8.4

Table 11. Observed characteristics of the two MFCs in this study.

Acknowledgements

Author details

Reuben Y. Tamakloe

Address all correspondence to: rionty@gmail.com

Department of Physics, KNUST, Kumasi, Ghana

References

[1] Bond DR, Holmes DE, Tender LM, Lovley DR. Electrode-reducing microorganisms that harvest energy from marine sediments. Science. 2002;**295**:483-485

[2] Patra A. Low-cost, single-chambered microbial fuel cells for harvesting energy and cleansing wastewater. Journal of the U.S. SJWP. 2008:72-82. Water Environment Federation. DOI: 10.2175/SJWP

[3] Samsudeen et al. Performance investigation of multi-chamber microbial fuel cell: An alternative approach for scale up system. Journal of Renewable and Sustainable Energy. July 2015;**7**(4). DOI: 10.1063/1.4923393

[4] Liu H, Logan B. Electricity generation using an air-cathode single chamber microbial fuel cell in the presence and absence of a proton exchange membrane. Environmental Science & Technology. 2004;**38**:4040-4046

[5] Cheng S, Logan BE. Increasing power generation for scaling up single-chamber air cathode microbial fuel cells. Bioresource Technology. 2011;**102**:4468-4473

[6] Zielke EA. Thermodynamic analysis of a single chamber microbial fuel. Cell. 2006

[7] Illumin. 2015. [Online] Available at: http://illumin.usc.edu/134/microbial-fuel-cells-generatingpower-from-waste/8-2-2015

[8] Zhao F, Robert CT Slade, JR Varcoe, Techniques for the study and development of microbial fuel cells: an electrochemical perspectiveChemical Sciences, University of Surrey, Guildford, GU2 7XH, United Kingdom, http://pubs.rsc.org/en/content/articlelaning/2009/cs/b819866g/unauth#! 17-04-2014

[9] Tamakloe RY, Singh K, Opoku-Donkor T. H_2O_2 as electron acceptor in double chamber microbial fuel cells. International Journal of Advanced Research in Engineering and Technology. 2014, January 2014;**5**(1):01-06

[10] Logan BE. Microbial Fuel Cells. 1st ed. U.S.A: John Wiley and Sons Inc; 2008. pp. 32-44

[11] Halliday D, Resnick R, Walker J. Extended Fundamentals of Physics. 2010 African Reprint. John Wiley & Sons Co: ISBN 978-81-265-0823-5. p. 640

[12] Pant D et al. A review of the substrates used in microbial fuel cells (MFCs) for sustainable energy production. Bioresource Technology. 2009. DOI: 10.1016/j.biortech.2009.10.017

[13] Tamakloe RY, Agamasu H, Singh K. International Journal of Advanced Research in Engineering and Technology (IJARET). July 2014;**5**(7):30-38; ISSN 0976 – 6480(Print), ISSN 0976 – 6499(Online) © IAEME

[14] Wei J, Liang P, Huang X. Recent progress in electrodes for microbial fuel cells. Bioresource Technology. 2011;**102**:9335-9344 www.elsevier.com/locate/biortech

[15] Folivi LE, Godman A, New Certificate Physics. Pub: Longman Group Ltd; 1977. pp. 310-314

[16] Opoku-Donkor T, Tamakloe RY, Nkum RK, Singh K. Effect of Cod on OCV, power production and coulombic efficiency of single-chambered microbial fuel cells. International Journal of Advanced Research in Engineering & Technology (IJARET). 2013;**4**(7):198-206, ISSN Print: 0976-6480, ISSN Online: 0976-6499

[17] Rabaey K, Verstraete W. Microbial fuel cells: Novel biotechnology for energy generation. Trends in Biotechnology. June 2005;**23**(6)